

## Abstract

1 We introduce *frequency propagation*, a learning algorithm for nonlinear physical  
2 networks. In a resistive electrical circuit with variable resistors, an activation cur-  
3 rent is applied at a set of input nodes at one frequency, and an error current is  
4 applied at a set of output nodes at another frequency. The voltage response of  
5 the circuit to these boundary currents is the superposition of an ‘activation signal’  
6 and an ‘error signal’ whose coefficients can be read in different frequencies of the  
7 frequency domain. Each conductance is updated proportionally to the product of  
8 the two coefficients. The learning rule is local and proved to perform gradient  
9 descent on a loss function. We argue that frequency propagation is an instance of  
10 a *multi-mechanism learning* strategy for physical networks, be it resistive, elastic,  
11 or flow networks. Multi-mechanism learning strategies incorporate at least two  
12 physical quantities, potentially governed by independent physical mechanisms, to  
13 act as activation and error signals in the training process. Locally available infor-  
14 mation about these two signals is then used to update the trainable parameters to  
15 perform gradient descent. We demonstrate how earlier work implementing learn-  
16 ing via *chemical signaling* in flow networks ([1]) also falls under the rubric of  
17 multi-mechanism learning.

## 18 Frequency propagation: Multi-mechanism learning in nonlinear physical 19 networks

### 20 I. INTRODUCTION

21 Advancements in artificial neural networks (ANN) ([2]) have inspired a search for adaptive phys-  
22 ical networks that can be optimized to achieve desired functionality ([1, 3–9]). Similar to ANNs,  
23 adaptive physical networks modify their learning degrees of freedom to approximate a desired input-  
24 to-output function ; but unlike ANNs, they achieve this using physical laws. In a physical network,  
25 the input is typically an externally applied boundary condition, and the output is the network’s re-  
26 sponse to this input, or a statistic of this response. For instance, in a resistive network, an input  
27 signal can be fed in the form of applied currents or voltages, and the output may be the vector of  
28 voltages across a subset of nodes of the network. The learning degrees of freedom of the network  
29 are, for example, the conductances of the resistors (assuming variable resistors). Ideally, these learn-  
30 ing parameters must be updated using only locally available information. Otherwise, the network  
31 would require additional channels to transmit the gradient information. Moreover, these parameter  
32 updates should preferably follow the direction of gradient descent in the loss function landscape, as  
33 is the case for ANNs.

34  
35 Existing learning algorithms for adaptive physical networks include *equilibrium propagation* ([3,  
36 10]) and *coupled learning* ([5]). These algorithms are based on the idea of *contrastive learning*  
37 ([11]) and proceed as follows. In a first phase, an input is presented to the network, either in the  
38 form of boundary currents or voltages, and the network is allowed to settle to equilibrium (the ‘free  
39 state’), where a supervisor checks the output of the system. Then the supervisor *nudges* the output  
40 towards the desired output. This perturbation causes the system to settle to a new (‘perturbed’)   
41 equilibrium state, which is a slightly more accurate approximation of the function that one wants to  
42 learn. The supervisor then compares the perturbed state with the free state to make changes in the  
43 learning degrees of freedom in such a way that the network spontaneously produces an output that  
44 is slightly closer to the desired output. In the limit of infinitesimal nudging, this procedure performs  
45 gradient descent on the squared prediction error ([12]).

46 The above procedure is not entirely ‘physical’ in nature, as it requires storing the free state to com-  
47 pare it with the perturbed state. For example, in the experimental work of [7], the authors use two  
48 copies of the same network to compute the two states. Alternatively, [13] use a single network,  
49 but the authors make use of additional SRAM to store the two states before performing the weight  
50 updates. Another idea proposed by [3] is to use a capacitor (sample-and-hold amplifier) at each

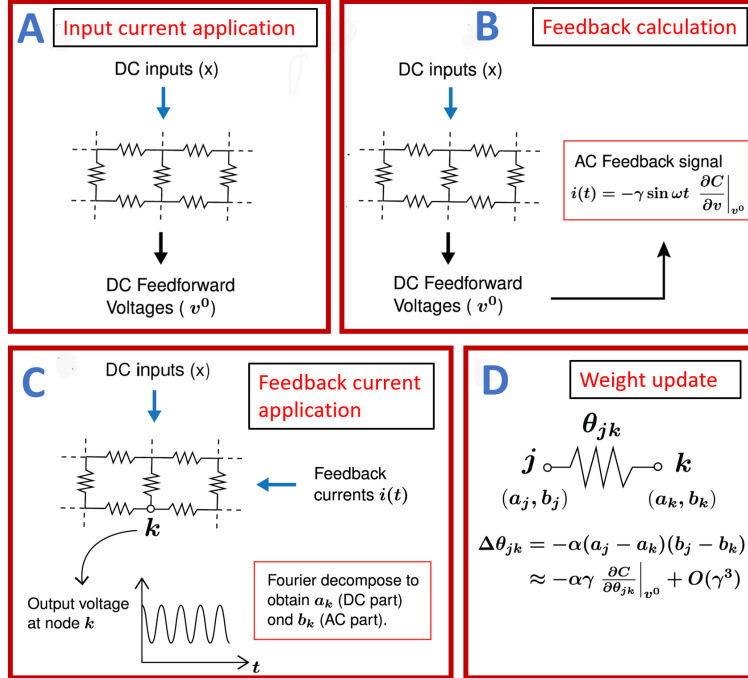


FIG. 1. A graphical summary of Frequency Propagation.

51 node/unit/neuron to store the free state values, but this idea has not been verified experimentally. In  
 52 this work, we propose an alternative *multi-mechanism learning* approach to overcome this hurdle.  
 53 Our approach incorporates two physical quantities, each driven by their own respective mechanisms:  
 54 one quantity acting as an *activation* signal and the other acting as an *error* signal. This concept  
 55 is motivated by biological systems implementing functionality via multiple biophysical routes or  
 56 mechanisms. Such functionality can be chemical, electrical or even mechanical in nature with po-  
 57 tential interactions between such mechanisms. For instance, in the brain, activity can propagate  
 58 from one cell to another via electrical and chemical synapses, as opposed to just one mechanism,  
 59 if you will ([14]). Given this modularity in functionality in biology, it would be remiss not to ex-  
 60 plore such richness in how adaptive physical networks learn. Alternatively, as we shall soon see, the  
 61 modularity is not necessarily in terms of mechanical versus chemical versus electrical signals, but  
 62 distinguishable signals.

63 We introduce *frequency propagation* (Freq-prop), a physical learning algorithm falling under the  
 64 umbrella concept of multi-mechanism learning. In Freq-prop, the activation and error signals are  
 65 both sent through a single channel, but are encoded in different frequencies of the frequency domain  
 66 ; we can thus obtain the respective responses of the system through frequency (Fourier) decompo-  
 67 sition. This algorithm, which we show to perform gradient descent, can be used to train adaptive  
 68 non-linear networks such as resistor networks, elastic networks and flow networks. Freq-prop thus  
 69 has the potential to be an all-encompassing approach. See Fig. 1 for a graphical summary of Freq-  
 70 prop. In the next section we present this idea of frequency propagation in the context of resistor  
 71 networks, and in section III we show that frequency propagation is an example of multi mecha-  
 72 nism learning and can be generalized to train various physical systems like flow and mechanical  
 73 networks.

## 74 II. NONLINEAR RESISTIVE NETWORKS

75 A resistive network is an electrical circuit of nodes interconnected by resistive devices, which in-  
 76 cludes linear resistors and diodes. Let  $N$  be the number of nodes in the network, and denote  $v_j$  the  
 77 electric potential of node  $j$ . A subset of the nodes are *input nodes*, where we can set input currents:  
 78 we denote  $x_j$  the input current at input node  $j$ . For each pair of nodes  $j$  and  $k$ , we denote  $\theta_{jk}$  the  
 79 conductance of the resistor between these nodes (provided that the corresponding branch contains

80 a linear resistor). We further denote  $\theta = \{\theta_{jk} : \text{linear branch } (j, k)\}$  the vector of conductances,  
 81 and  $x = (x_1, x_2, \dots, x_N)$  the vector of input currents, where by convention  $x_j = 0$  if node  $j$  is  
 82 not an input node. Finally, we denote  $v = (v_1, v_2, \dots, v_N)$  the configuration of the nodes' electric  
 83 potentials, and  $v(\theta, x)$  the equilibrium value of  $v$  as a function of the branch conductances ( $\theta$ ) and  
 84 the input currents ( $x$ ).

85 The following result, known since the work of Millar ([15]), provides a characterization of the  
 86 equilibrium state – see also ([3]) for a proof of this result with notations closer to ours.

87 **Theorem 1** *There exists a real-valued function  $E(\theta, x, v)$  such that*

$$v(\theta, x) = \arg \min_v E(\theta, x, v). \quad (1)$$

88 *Furthermore,  $E(\theta, x, v)$  is of the form*

$$E(\theta, x, v) = E_{\text{input}}(x, v) + E_{\text{nonlinear}}(v) \quad (2)$$

$$+ \sum_{\text{linear branch } (j,k)} \frac{1}{2} \theta_{jk} (v_j - v_k)^2, \quad (3)$$

89 *where  $E_{\text{input}}(x, v)$  is a function of  $x$  and  $v$ , and  $E_{\text{nonlinear}}(v)$  is a function of  $v$  only.*

90  $E(\theta, x, v)$  is the ‘energy function’ of the system, also called the *co-content* ([15]), and the equilib-  
 91 rium state  $v(\theta, x)$  is a minimizer of the energy function. The energy function contains an energy  
 92 term  $E_{\text{input}}(x, v)$  associated to boundary input currents  $x$ . It also contains energy terms of the form  
 93  $\theta_{jk} (v_j - v_k)^2$  representing the power dissipated in branch  $(j, k)$ . The term  $E_{\text{nonlinear}}(v)$  contains  
 94 all nonlinearities of the system. In a *linear* resistance network (i.e. when  $E_{\text{nonlinear}}(v) = 0$ ), it  
 95 is well known that the equilibrium configuration of node electric potentials minimizes the power  
 96 dissipation ; Theorem 1 generalizes this result to nonlinear networks. Below we explain how the  
 97 different terms of  $E(\theta, x, v)$  are constructed.

98 **Constructing the energy function.** Each branch is characterised by its current-voltage character-  
 99 istic  $i_{jk} = \widehat{i}_{jk}(v_j - v_k)$ , where  $\widehat{i}_{jk}(\cdot)$  is a real-valued function that returns  $i_{jk}$ , the current flowing  
 100 from  $j$  to  $k$  in response to the voltage  $v_j - v_k$ . The energy term corresponding to branch  $(j, k)$ ,  
 101 called the *co-content* of the branch ([15]), is by definition

$$E_{jk}(v_j - v_k) = \int_0^{v_j - v_k} \widehat{i}_{jk}(v') dv'. \quad (4)$$

102 In general, the characteristic function  $\widehat{i}_{jk}(\cdot)$  is arbitrary, i.e. *nonlinear*. However, some branches are  
 103 *linear*, meaning that their current-voltage characteristic is of the form  $i_{jk} = \theta_{jk} (v_j - v_k)$ , where  
 104  $\theta_{jk}$  is the branch conductance [16]. For such linear branches, the energy term is

$$E_{jk}(v_j - v_k) = \frac{1}{2} \theta_{jk} (v_j - v_k)^2, \quad (5)$$

105 which is the power dissipated in branch  $(j, k)$ .

106 We gather all the energy terms of nonlinear branches under a unique term:

$$E_{\text{nonlinear}}(v) = \sum_{\text{nonlinear branch } (j,k)} E_{jk}(v_j - v_k), \quad (6)$$

107 where we recall that  $v = (v_1, v_2, \dots, v_N)$ .

108 As for the energy term  $E_{\text{input}}(x, v)$ , we present two ways to impose boundary conditions to the  
 109 network to feed it with input signals  $x$ , either in the form of boundary currents or boundary electric  
 110 potentials. Recall that we write  $x = (x_1, x_2, \dots, x_N)$  the vector of input signals, where  $x_j = 0$  if  
 111 node  $j$  is not an input node. In the case of boundary currents, the corresponding energy term is

$$E_{\text{input}}^{\text{current}}(x, v) = \sum_{j \in \{\text{input nodes}\}} x_j v_j, \quad (7)$$

112 whereas in the case of boundary electric potentials, the energy term is

$$E_{\text{input}}^{\text{voltage}}(x, v) = \begin{cases} 0 & \text{if } v_j = x_j, \\ \forall j \in \{\text{input nodes}\}, \\ +\infty & \text{otherwise,} \end{cases} \quad (8)$$

113 i.e. the electric potential  $v_j$  is clamped to  $x_j$  for every input node  $j$  (so that the energy remains  
114 finite).

115 Putting all the energy terms together, and denoting  $E_{\text{input}}(x, v)$  the energy term of input signals  
116 (either  $E_{\text{input}}^{\text{current}}(x, v)$  or  $E_{\text{input}}^{\text{voltage}}(x, v)$  depending on the case), we get the energy function of Eq. (2-  
117 3).

### 118 III. MULTI-MECHANISM LEARNING VIA FREQUENCY 119 PROPAGATION

120 Learning in a resistive network consists in adjusting the branch conductances ( $\theta$ ) so that the network  
121 exhibits a desired behavior, i.e. a desired input-output function  $x \mapsto v(\theta, x)$ . In machine learning,  
122 this problem is formalized by introducing a *cost function*  $C$ . Given an input-output pair  $(x, y)$ ,  
123 the quantity  $C(v(\theta, x), y)$  measures the discrepancy between the ‘model prediction’  $v(\theta, x)$  and the  
124 desired output  $y$ . The learning objective is to find the parameters  $\theta$  that minimize the expected cost  
125  $\mathbb{E}_{(x,y)} [C(v(\theta, x), y)]$  over input-output pairs  $(x, y)$  coming from the data distribution for the task  
126 that the system must solve.

127 In deep learning, the main tool for this optimization problem is stochastic gradient descent  
128 (SGD) ([17]): at each step we pick at random an example  $(x, y)$  from the training set and update the  
129 parameters as

$$\Delta\theta = -\eta \frac{\partial \mathcal{L}}{\partial \theta}(\theta, x, y), \quad (9)$$

130 where  $\eta$  is a step size, and

$$\mathcal{L}(\theta, x, y) = C(v(\theta, x), y) \quad (10)$$

131 is the per-example *loss function*.

132 We now present *frequency propagation* (Freq-prop), a learning algorithm for physical networks  
133 whose update rule performs SGD. Freq-prop proceeds by modifying the energy of the network  
134 to push or pull away the network’s output values from the desired outputs. In the case of a  
135 resistive network (Section II), we inject sinusoidal currents at the output nodes of the network,  
136  $i(t) = \gamma \sin(\omega t) \frac{\partial C}{\partial v}(v, y)$ , where  $t$  denotes time,  $\omega$  is a frequency, and  $\gamma$  is a small positive  
137 constant[18]. This amounts to augment the energy function of the system by a time-dependent  
138 sinusoidal energy term  $\gamma \sin(\omega t) C(v, y)$ . Due to this perturbation, the system’s response  $v(t)$  min-  
139 imizing the energy at time  $t$  is

$$v(t) = \arg \min_v [E(\theta, x, v) + \gamma \sin(\omega t) C(v, y)]. \quad (11)$$

140 The response  $v(t)$  is periodic of period  $T = 2\pi/\omega$ , and for small perturbations (i.e.  $\gamma \ll 1$ ), it  
141 is approximately sinusoidal. Next, we assume that we can recover the first two vectors of Fourier  
142 coefficients of  $v(t)$ , i.e. the vectors  $a$  and  $b$  such that

$$a = \frac{1}{T} \int_0^T v(t) dt, \quad b = \frac{2}{T} \int_0^T v(t) \sin(\omega t) dt. \quad (12)$$

143 Finally, denoting  $a = (a_1, a_2, \dots, a_N)$  and  $b = (b_1, b_2, \dots, b_N)$ , we update each parameter  $\theta_{jk}$   
144 according to the learning rule

$$\Delta\theta_{jk} = -\alpha (b_j - b_k) \cdot (a_j - a_k), \quad (13)$$

145 where  $\alpha$  is a positive constant.

146 **Theorem 2** For every parameter  $\theta_{jk}$ , we have

$$\Delta\theta_{jk} = -\alpha \gamma \frac{\partial \mathcal{L}}{\partial \theta_{jk}}(\theta, x, y) + O(\gamma^3) \quad (14)$$

147 when  $\gamma \rightarrow 0$ .

148 Namely, the learning rule (13) approximates one step of gradient descent with respect to the loss,  
 149 with learning rate  $\alpha\gamma$ . Note that this learning rule is local: it requires solely locally available  
 150 information for each parameter  $\theta_{jk}$ .

151 [Proof of Theorem 2] Let  $\theta$ ,  $x$  and  $y$  be fixed. For every  $\beta \in \mathbb{R}$ , we denote

$$v_{\star}^{\beta} = \arg \min_v [E(\theta, x, v) + \beta C(v, y)]. \quad (15)$$

152 With this notation, note that the response  $v(t)$  of Eq. (11) rewrites  $v(t) = v_{\star}^{\gamma \sin(\omega t)}$ . Let us write the  
 153 second-order Taylor expansion of  $v_{\star}^{\beta}$  around  $\beta = 0$ :

$$v_{\star}^{\beta} = v_{\star}^0 + \beta \left. \frac{\partial v_{\star}^{\beta}}{\partial \beta} \right|_{\beta=0} + \frac{\beta^2}{2} \left. \frac{\partial^2 v_{\star}^{\beta}}{\partial \beta^2} \right|_{\beta=0} + O(\beta^3), \quad (16)$$

154 where  $v_{\star}^0 = v(\theta, x)$  by definition (1), and  $\left. \frac{\partial v_{\star}^{\beta}}{\partial \beta} \right|_{\beta=0}$  and  $\left. \frac{\partial^2 v_{\star}^{\beta}}{\partial \beta^2} \right|_{\beta=0}$  denote the derivative and second-  
 155 derivative of  $v_{\star}^{\beta}$  at  $\beta = 0$ . Taking  $\beta = \gamma \sin(\omega t)$  in the above formula, we get

$$v(t) = v_{\star}^{\gamma \sin(\omega t)} = v_{\star}^0 + \gamma \sin(\omega t) \left. \frac{\partial v_{\star}^{\beta}}{\partial \beta} \right|_{\beta=0} \quad (17)$$

$$+ \frac{\gamma^2}{2} \sin(\omega t)^2 \left. \frac{\partial^2 v_{\star}^{\beta}}{\partial \beta^2} \right|_{\beta=0} + O(\gamma^3), \quad (18)$$

156 uniformly in  $t$ . Therefore, the first two vectors of Fourier coefficients  $a$  and  $b$  of the periodic function  
 157  $v(t)$ , with time period  $T = 2\pi/\omega$  are

$$a = \frac{1}{T} \int_0^T v(t) dt = v_{\star}^0 + \frac{\gamma^2}{4} \left. \frac{\partial^2 v_{\star}^{\beta}}{\partial \beta^2} \right|_{\beta=0} + O(\gamma^3), \quad (19)$$

$$b = \frac{2}{T} \int_0^T v(t) \sin(\omega t) dt = \gamma \left. \frac{\partial v_{\star}^{\beta}}{\partial \beta} \right|_{\beta=0} + O(\gamma^3). \quad (20)$$

158 Next, we know from the equilibrium propagation formula (Theorem 2.1 in ([10])) that the gradient  
 159 of the loss  $\mathcal{L}$  is equal to

$$\frac{\partial \mathcal{L}}{\partial \theta}(\theta, x, y) = \left. \frac{d}{d\beta} \right|_{\beta=0} \frac{\partial E}{\partial \theta}(\theta, x, v_{\star}^{\beta}). \quad (21)$$

160 Therefore,

$$\frac{\partial \mathcal{L}}{\partial \theta}(\theta, x, y) = \frac{\partial^2 E}{\partial \theta \partial v}(\theta, x, v_{\star}^0) \cdot \left. \frac{\partial v_{\star}^{\beta}}{\partial \beta} \right|_{\beta=0}. \quad (22)$$

161 Multiplying both sides by  $\gamma$ , and using (20), we get

$$\gamma \frac{\partial \mathcal{L}}{\partial \theta}(\theta, x, y) = \frac{\partial^2 E}{\partial \theta \partial v}(\theta, x, v_{\star}^0) \cdot b + O(\gamma^3). \quad (23)$$

162 Finally, given the form of the energy function (2), and using  $b = O(\gamma)$  and  $v_{\star}^0 = a + O(\gamma^2)$  from  
 163 Eq. (19), we get for every parameter  $\theta_{jk}$

$$\gamma \frac{\partial \mathcal{L}}{\partial \theta_{jk}}(\theta, x, y) = (a_j - a_k) \cdot (b_j - b_k) + O(\gamma^3). \quad (24)$$

164 Therefore the learning rule

$$\Delta \theta_{jk} = -\alpha (b_j - b_k) \cdot (a_j - a_k) \quad (25)$$

165 satisfies

$$\Delta \theta_{jk} = -\alpha \gamma \frac{\partial \mathcal{L}}{\partial \theta_{jk}}(\theta, x, y) + O(\gamma^3). \quad (26)$$

166 Hence the result.

167 **Remark 1.** For simplicity, we have omitted the time of relaxation to equilibrium in our analysis.  
 168 However, a practical circuit has an effective capacitance  $C_{\text{eff}}$  and therefore will equilibrate in time  
 169  $\tau_{\text{relax}} \sim R_{\text{eff}}C_{\text{eff}}$ , where  $R_{\text{eff}}$  is the effective resistance of the circuit. Our learning algorithm will  
 170 work as long as the circuit equilibrates much faster than the timescale of oscillation ( $\tau_{\text{relax}} \ll 1/\omega$ ).  
 171 Our analysis thus requires that  $C_{\text{eff}}$  be small enough for the assumption  $\tau_{\text{relax}} \ll 1/\omega$  to hold. If this  
 172 is not the case, there will be a tradeoff between how fast one can train the network with Freq-Prop vs  
 173 how accurate the approximation is for gradient. We leave the study of the regime where  $C_{\text{eff}}$  is non  
 174 negligible for future work. We note however that the effective capacitance of the circuit is expected  
 175 to grow linearly with the size of the network (the total amount of wire), so that inference time  
 176 grows linearly with the size of the network, too. We also note that the same is true for deep neural  
 177 networks: in a feedforward network, both inference (the forward pass) and training (the backward  
 178 pass of backpropagation) grow linearly with the size of the network.

179 **Remark 2.** While our nudging method (11) is inspired by the one of *equilibrium propagation*  
 180 ([3, 12]), it is also possible to apply the nudging variant of *coupled learning* ([5]) which might be  
 181 easier to implement in practice ([7]). To do this, we denote  $v_O^F$  the ‘free’ equilibrium value of the  
 182 output nodes of the network (where the prediction is read), without nudging. Then, at time  $t$ , we  
 183 *clamp* the output nodes to  $v_O^C(t) = v_O^F + \gamma \sin(\omega t)(y - v_O^F)$ . This nudging method can be achieved  
 184 via AC voltage sources at output nodes. We note however that Theorem 2 does not hold with this  
 185 alternative nudging method.

186 **Remark 3.** Measuring  $b_j$  for every node  $j$  as per Eq. (12) requires that we use the same reference  
 187 time  $t = 0$  for all nodes, i.e. it requires global synchronization of the measurements for all nodes.  
 188 However, in practice, there may be a time delay  $t_j$  between nudging and measurement, leading to a  
 189 measured response  $v_j(t) = a_j + b_j \sin(\omega(t+t_j)) + O(\gamma^3)$  at node  $j$ . Without any information about  
 190  $t_j$ , we can only obtain the absolute value of the coefficient  $b_j$ , not its sign. We propose a solution to  
 191 this issue in Appendix A.

## 192 IV. DISCUSSION

193 We have introduced frequency propagation (Freq-prop), a physical learning algorithm that falls in  
 194 the category of Multi-mechanism Learning (MmL). In MmL, separate and “distinguishable” acti-  
 195 vation and error signals both contribute to a local learning rule, such that trainable parameters (e.g.  
 196 conductances of variable resistors) perform gradient descent on a loss function. In Freq-prop, the  
 197 activation and error signals are implemented using different frequencies of a single physical quantity  
 198 (e.g. voltages or currents) and are thus distinguishable. We note however that the ‘distinguishabil-  
 199 ity’ of the signals does not mean that they are mathematically ‘independent’: in Freq-prop, the error  
 200 signal depends on the activation signal via the Hessian of the network. Other potential MmL algo-  
 201 rithms may involve independent physical mechanisms, such as an electrical activation signal and a  
 202 chemical error signal or vice versa. Multi-mechanism learning algorithms, such as Freq-prop, may  
 203 have implications towards designing fast and low-power, or high-efficiency, hardware for AI, as they  
 204 are rooted in physical principles. For the time being, inroads are being made by using backpropaga-  
 205 tion to train controllable physical systems in a hybrid *in silico-in situ* approach ([19]). As we work  
 206 towards a fully *in situ* approach, Freq-prop is a natural candidate. And while the *in situ* realization  
 207 of a nonlinear resistor network is an obvious starting point, there are potential limitations, particu-  
 208 larly in terms of timescales. Consider the time of relaxation to equilibrium ( $\tau_{\text{relax}}$ ), the time scale of  
 209 the sinusoidal nudging signal ( $T = 2\pi/\omega$ ), and the time scale of learning ( $\tau_{\text{learning}}$ ). Our learning  
 210 methodology requires that  $\tau_{\text{relax}} \ll T < \tau_{\text{learning}}$ . More specifically,

- 211 1. Once input is applied, the network reaches equilibrium in time  $\tau_{\text{relax}}$ .
- 212 2. Based on the network’s output, a sinusoidal nudging signal of frequency  $\omega$  is applied at the  
 213 output nodes. The time scale of evolution of this sinusoidal nudging wave is  $T = 2\pi/\omega$ .  
 214 Assuming that  $\tau_{\text{relax}} \ll T$ , the network is at equilibrium at every instant  $t$ .
- 215 3. We observe the network’s response  $v(t)$  for a time  $\tau_{\text{obs}} > T$  to extract the coefficients  $a$   
 216 and  $b$  of Eq. (12). Updating the conductances of the resistors takes a time  $\tau_{\text{learning}} \sim \tau_{\text{obs}}$   
 217 using the values of  $a$  and  $b$  to determine the magnitude and sign of these updates.

218 Finally, could something like Freq-prop occur in the brain? Earlier work analyzing local field po-  
 219 tentials recorded simultaneously from different regions in the cortex suggested that feedforward

220 signaling is carried by gamma-band (30–80 Hz) activity, whereas feedback signaling is mediated  
 221 by alpha-(5–15Hz) or beta- (14–18 Hz) band activity, though local field potentials are not actively  
 222 relayed between regions ([20]). More recent work in the visual cortex argues that feedforward and  
 223 feedback signaling rely on separate “channels” since correlations in neuronal population activity  
 224 patterns, which are actively relayed between regions, are distinct during feedforward- and feedback-  
 225 dominated periods ([21]). Freq-prop is also related in spirit to the idea of frequency multiplexing  
 226 in biological neural networks ([22–24]), which uses the simultaneous encoding of two or more sig-  
 227 nals. While Freq-prop here uses only two separate signals – an activation signal and an error signal  
 228 – one can envision multiple activation and error signals being encoded to accommodate vector in-  
 229 puts and outputs and to accommodate multiple, competing cost functions. With multiple activation  
 230 and error signals one can also envision coupling learning via chemical signaling (Appendix D) with  
 231 Freq-prop, for example, to begin to capture the full computational *creativity* of the brain.

## 232 ACKNOWLEDGMENTS

233 The authors thank Sam Dillavou, Nachi Stern, Andrea Liu, Doug Durian, and Jack Kendall for dis-  
 234 cussion. JMS acknowledges financial support from NSF-DMR-1832002 and NSF-DMR-2204312.

- 
- 235 [1] V. R. Anisetti, B. Scellier, and J. M. Schwarz, “Learning by non-interfering feedback chemical signaling  
 236 in physical networks,” *arXiv preprint arXiv:2203.12098*, 2022.
- 237 [2] I. Goodfellow, Y. Bengio, and A. Courville, *Deep learning*. MIT press, 2016.
- 238 [3] J. Kendall, R. Pantone, K. Manickavasagam, Y. Bengio, and B. Scellier, “Training end-to-end analog  
 239 neural networks with equilibrium propagation,” *arXiv preprint arXiv:2006.01981*, 2020.
- 240 [4] M. Stern, C. Arinze, L. Perez, S. E. Palmer, and A. Murugan, “Supervised learning through physical  
 241 changes in a mechanical system,” Jun 2020.
- 242 [5] M. Stern, D. Hexner, J. W. Rocks, and A. J. Liu, “Supervised learning in physical networks: From machine  
 243 learning to learning machines,” *Physical Review X*, vol. 11, no. 2, p. 021045, 2021.
- 244 [6] V. Lopez-Pastor and F. Marquardt, “Self-learning machines based on hamiltonian echo backpropagation,”  
 245 *arXiv preprint arXiv:2103.04992*, 2021.
- 246 [7] S. Dillavou, M. Stern, A. J. Liu, and D. J. Durian, “Demonstration of decentralized, physics-driven learn-  
 247 ing,” *arXiv preprint arXiv:2108.00275*, 2021.
- 248 [8] B. Scellier, S. Mishra, Y. Bengio, and Y. Ollivier, “Agnostic physics-driven deep learning,” *arXiv preprint*  
 249 *arXiv:2205.15021*, 2022.
- 250 [9] M. Stern and A. Murugan, “Learning without neurons in physical systems,” 2022.
- 251 [10] B. Scellier, *A deep learning theory for neural networks grounded in physics*. PhD thesis, Université de  
 252 Montréal, 2021.
- 253 [11] P. Baldi and F. Pineda, “Contrastive learning and neural oscillations,” *Neural computation*, vol. 3, no. 4,  
 254 pp. 526–545, 1991.
- 255 [12] B. Scellier and Y. Bengio, “Equilibrium propagation: Bridging the gap between energy-based models and  
 256 backpropagation,” *Frontiers in computational neuroscience*, vol. 11, p. 24, 2017.
- 257 [13] S.-i. Yi, J. D. Kendall, R. S. Williams, and S. Kumar, “Activity-difference training of deep neural networks  
 258 using memristor crossbars,” *Nature Electronics*, vol. 6, no. 1, pp. 45–51, 2023.
- 259 [14] A. E. Pereda, “Electrical synapses and their functional interactions with chemical synapses,” *Nature Re-*  
 260 *views Neuroscience*, vol. 15, no. 4, pp. 250–263, 2014.
- 261 [15] W. Millar, “Cxvi. some general theorems for non-linear systems possessing resistance,” *The London,*  
 262 *Edinburgh, and Dublin Philosophical Magazine and Journal of Science*, vol. 42, no. 333, pp. 1150–1160,  
 263 1951.
- 264 [16] To avoid any confusion, we stress that  $\theta_{jk}$  is a scalar, whereas  $\hat{i}_{jk}(\cdot)$  is a real-valued function. Thus,  
 265  $\theta_{jk}(v_j - v_k)$  denotes the product of  $\theta_{jk}$  and  $v_j - v_k$ , whereas  $\hat{i}_{jk}(v_j - v_k)$  denotes the function  $\hat{i}_{jk}$   
 266 applied to the voltage  $v_j - v_k$ .
- 267 [17] L. Bottou, “Large-scale machine learning with stochastic gradient descent,” in *Proceedings of COMP-*  
 268 *STAT’2010*, pp. 177–186, Springer, 2010.
- 269 [18] In practical situations such as the squared error prediction, the cost function  $C$  depends only on the state  
 270 of output nodes ; therefore nudging requires injecting currents at output nodes only.
- 271 [19] L. G. Wright, T. Onodera, M. M. Stein, T. Wang, D. T. Schachter, Z. Hu, and P. L. McMahon, “Deep  
 272 physical neural networks trained with backpropagation,” *Nature*, vol. 601, no. 7894, pp. 549–555, 2022.
- 273 [20] A. M. Bastos, J. Vezoli, C. A. Bosman, J.-M. Schoffelen, R. Oostenveld, J. R. Dowdall, P. De Weerd,  
 274 H. Kennedy, and P. Fries, “Visual areas exert feedforward and feedback influences through distinct fre-

- 275 quency channels,” *Neuron*, vol. 85, no. 2, pp. 390–401, 2015.
- 276 [21] J. D. Smedo, A. I. Jasper, A. Zandvakili, A. Krishna, A. Aschner, C. K. Machens, A. Kohn, and B. M.
- 277 Yu, “Feedforward and feedback interactions between visual cortical areas use different population activity
- 278 patterns,” *Nature communications*, vol. 13, no. 1, pp. 1–14, 2022.
- 279 [22] R. Naud and H. Sprekeler, “Sparse bursts optimize information transmission in a multiplexed neural code,”
- 280 *Proceedings of the National Academy of Sciences*, vol. 115, no. 27, pp. E6329–E6338, 2018.
- 281 [23] A. Payeur, J. Guerguiev, F. Zenke, B. A. Richards, and R. Naud, “Burst-dependent synaptic plasticity can
- 282 coordinate learning in hierarchical circuits,” *Nature neuroscience*, vol. 24, no. 7, pp. 1010–1019, 2021.
- 283 [24] T. Akam and D. M. Kullmann, “Oscillatory multiplexing of population codes for selective communication
- 284 in the mammalian brain,” Jan 2014.
- 285 [25] C. Cherry, “Cxvii. some general theorems for non-linear systems possessing reactance,” *The London,*
- 286 *Edinburgh, and Dublin Philosophical Magazine and Journal of Science*, vol. 42, no. 333, pp. 1161–1177,
- 287 1951.
- 288 [26] J. J. Hopfield, “Neurons with graded response have collective computational properties like those of two-
- 289 state neurons.,” *Proceedings of the national academy of sciences*, vol. 81, no. 10, pp. 3088–3092, 1984.
- 290 [27] A. Laborieux and F. Zenke, “Holomorphic equilibrium propagation computes exact gradients through
- 291 finite size oscillations,” *Advances in Neural Information Processing Systems*, vol. 35, pp. 12950–12963,
- 292 2022.
- 293 [28] N. Zucchet and J. Sacramento, “Beyond backpropagation: implicit gradients for bilevel optimization,”
- 294 *arXiv preprint arXiv:2205.03076*, 2022.

## 295 Appendix A: Choice of the nudging signal

296 We have seen in section III that, using a sinusoidal nudging signal  $\gamma \sin(\omega t) C(v, y)$ , the measured

297 response at node  $j$  will be of the form  $v_j(t) = a_j + b_j \sin(\omega(t + t_j)) + O(\gamma^3)$ , where  $t_j$  is the time

298 delay between nudging and measurement. Unfortunately, it is not possible to recover the sign of  $b_j$

299 without any knowledge of  $t_j$ . This problem can be overcome by using a different nudging signal.

300 In general, if we nudge the system by an energy term  $\gamma f(t) C(v, y)$ , where  $f(t)$  is an arbitrary

301 function such that  $\sup_t |f(t)| < \infty$ , then the system’s response at node  $j$  will be of the form  $v_j(t) =$

302  $a_j + b_j f(t + t_j) + O(\gamma^2)$ . Our goal is to choose a  $f$  so that we can obtain for every node  $j$  the

303 values of  $a_j$  and  $b_j$  by measuring only  $v_j(t)$ , without knowing  $t_j$ .

304 Clearly, this is not possible for all functions  $f$ . For example, if  $f(\cdot)$  is a constant, then  $v_j(\cdot)$  is also

305 a constant, and we cannot recover the values of  $a_j$  and  $b_j$  from  $v_j(\cdot)$  alone. As seen above, another

306 example for which this is not possible is  $f(t) = \sin(\omega t)$ . This is because a time delay  $t_j = \pi/\omega$

307 will change the sign of the signal,  $\sin(\omega(t + t_j)) = -\sin(\omega t)$ ; therefore the sign of  $b_j$  cannot be

308 recovered without any knowledge of  $t_j$ .

309 An example of a nudging signal for which we can infer the values of  $a_j$  and  $b_j$  (up to  $O(\gamma^2)$ ) is

310  $f(t) = |\sin(\omega(t))|$ . To do this, we observe the response at node  $j$

$$v_j(t) = a_j + b_j |\sin(\omega(t + t_j))| + O(\gamma^2) \quad (\text{A1})$$

311 for a duration  $\tau_{\text{obs}}$  greater than the time period of the signal  $T = 2\pi/\omega$ . The coefficients  $a_j$  and

312  $b_j$  can be obtained by identifying the times where the signal’s derivative is zero or is discontinuous.

313 Specifically, denoting  $\partial_+ v_j(t)$  and  $\partial_- v_j(t)$  the left and right derivatives of the signal at time  $t$ , we

314 have

$$a_j = v_j(t_1) + O(\gamma^2) \text{ where } \partial_+ v(t_1) \neq \partial_- v(t_1), \quad (\text{A2})$$

$$b_j = v_j(t_2) - v_j(t_1) + O(\gamma^2) \text{ where } \partial v(t_2) = 0. \quad (\text{A3})$$

315 More generally, we will show that, in principle, it is possible to recover the coefficients  $a_j$  and  $b_j$  if

316 and only if the function  $f$  has the property that there is no  $\tau$  such that  $f(t) = \sup f + \inf f - f(t + \tau)$

317 for every  $t$ . In other words, no amount of time delay converts the signal’s ‘upright’ form to its

318 ‘inverted’ form or vice versa.

319 Let  $f(t)$  denote the nudging signal. Assuming that  $f$  is bounded, recall that, for every  $j$ , the mea-

320 sured response  $v_j(t)$  at node  $j$  is of the form  $v_j(t) = a_j + b_j f(t + t_j) + O(\gamma^2)$ , where  $a_j$  and  $b_j$

321 are the numbers that we wish to recover (up to  $O(\gamma^2)$ ) to implement the parameter update, and  $t_j$  is

322 an unknown time delay. Our goal is to obtain for every node  $j$  the values of  $a_j$  and  $b_j$  by measuring

323 only  $v_j(t)$ , without any knowledge of  $t_j$ .

324 We now establish a necessary and sufficient condition on the nudging signal  $f(t)$  so that one can,  
 325 at least in principle, uniquely obtain the values of  $a_j$  and  $b_j$  for every node  $j$ . We are concerned  
 326 with quantities that depend only on a single node and hence we will drop the node index with the  
 327 understanding that all of the analysis applies to any arbitrary node.

328 Let  $F$  denote the set of all real-valued, bounded functions, and let  $f$  be an element of  $F$ . Let  
 329  $\mathcal{C}_f : \mathbb{R}^3 \rightarrow F$  be the function that maps the parameters  $(a, b, t_0)$  to the function  $v(\cdot) = a + bf(\cdot + t_0)$ .  
 330 We define the following equivalence relation on  $F$ : two functions  $g, h \in F$  are equivalent if they  
 331 differ by a time translation, i.e.,  $g \sim h$  if and only if there exists a  $t_0 \in \mathbb{R}$  such that  $g(t) = h(t + t_0)$   
 332 for all  $t \in \mathbb{R}$ . Let  $\tilde{F} = F / \sim$  be the quotient of  $F$  under this equivalence relation and let  $[g]$  be  
 333 the equivalence class that contains the function  $g$ . The map  $\mathcal{C}_f$  can be lifted to yield  $\tilde{\mathcal{C}}_f : \mathbb{R}^2 \rightarrow \tilde{F}$   
 334 such that  $\tilde{\mathcal{C}}_f(a, b) = [a + bf]$ . In order to be able to uniquely extract  $a$  and  $b$  from any equivalence  
 335 class of the form  $[a + bf]$ , the function  $\tilde{\mathcal{C}}_f$  has to be injective. This can be re-expressed as a direct  
 336 condition on the nudging signal  $f$ .

337 **Proposition 3** *The following statements are equivalent:*

338 *P1: The function  $\tilde{\mathcal{C}}_f : \mathbb{R}^2 \rightarrow \tilde{F}$  defined by  $\tilde{\mathcal{C}}_f(a, b) = [a + bf]$  is injective.*

339 *P2: There exists no  $\tau \in \mathbb{R}$  such that for all  $t \in \mathbb{R}$ ,*  
 340  $f(t) = \sup f + \inf f - f(t + \tau)$ .

341 where  $\sup f = \sup_t f(t)$  and  $\inf f = \inf_t f(t)$  denote the supremum and infimum values of the  
 342 nudging signal  $f$  respectively.

343 We establish this by proving that the negation of the two statements are equivalent, i.e., the following  
 344 statements are equivalent:

345 **N1:** There exists two distinct pairs of real numbers  $(a_1, b_1)$  and  $(a_2, b_2)$  such that  $[a_1 + b_1 f] =$   
 346  $[a_2 + b_2 f]$ .

347 **N2:** There exists a  $\tau \in \mathbb{R}$  such that for all  $t \in \mathbb{R}$ ,  
 348  $f(t) = \sup f + \inf f - f(t + \tau)$ .

349 Suppose that N2 is true: there is a  $\tau \in \mathbb{R}$  such that for all  $t \in \mathbb{R}$ ,  $f(t) = \sup f + \inf f - f(t + \tau)$ . This  
 350 means that  $f$  and  $\sup f + \inf f - f$  are related by a time translation, i.e.  $[f] = [\sup f + \inf f - f]$ .  
 351 Therefore, N1 is true, with  $(a_1, b_1) = (0, 1)$  and  $(a_2, b_2) = (\sup f + \inf f, -1)$ .

352 Conversely, suppose that N1 is true: there exists two distinct pairs of real numbers  $(a_1, b_1)$  and  
 353  $(a_2, b_2)$  and a  $\tau \in \mathbb{R}$  such that

$$\forall t \in \mathbb{R}, \quad a_1 + b_1 f(t) = a_2 + b_2 f(t + \tau). \quad (\text{A4})$$

354 The numbers  $b_1$  and  $b_2$  cannot be both zero, otherwise the above equation implies that  $a_1 = a_2$ , a  
 355 contradiction. If  $b_1 = 0$  and  $b_2 \neq 0$ , the above equation implies that  $f$  is a constant, in which case  
 356 N2 is clearly true. Otherwise  $b_1 \neq 0$  and we can re-write the above equality as

$$\forall t \in \mathbb{R}, \quad f(t) = a + bf(t + \tau) \quad (\text{A5})$$

357 with  $a = (a_2 - a_1)/b_1$  and  $b = b_2/b_1$ . Now there are two possibilities: either  $b > 0$  or  $b < 0$ .

358 First, let us suppose that  $b > 0$ . The above equality imposes the following conditions on the mini-  
 359 mum and maximum values of the function  $f$ :

$$\sup f = a + b \sup f, \quad (\text{A6})$$

$$\inf f = a + b \inf f. \quad (\text{A7})$$

360 Subtracting (A7) from (A6) and reorganizing the terms we get  $(1 - b)(\sup f - \inf f) = 0$ . If  $b = 1$ ,  
 361 then  $a = 0$ , contradicting our assumption that  $(a_1, b_1)$  and  $(a_2, b_2)$  are distinct pairs. Therefore  
 362  $\sup f = \inf f$ ,  $f$  is constant and N2 is true.

363 Second, let us suppose that  $b < 0$ . As before we have

$$\sup f = a + b \inf f, \quad (\text{A8})$$

$$\inf f = a + b \sup f, \quad (\text{A9})$$

364 and again  $(1 + b)(\sup f - \inf f) = 0$ . Either  $f$  is a constant, or  $b = -1$ , implying in turn that  
 365  $a = \sup f + \inf f$ . Therefore, coming back to (A5), we have  $f(t) = \sup f + \inf f - f(t + \tau)$  for  
 366 all  $t \in \mathbb{R}$ , which is the statement of N2.

## 367 Appendix B: General Applicability of Frequency Propagation

368 Freq-prop applies to arbitrary physical networks: not only resistive networks, but also flow net-  
 369 works, capacitive networks and inductive networks, among others. In these networks, the notion  
 370 of current-voltage characteristics will be replaced by current-pressure characteristics, current-flux  
 371 characteristics, and charge-voltage characteristics, respectively. The mathematical framework for  
 372 nonlinear elements (Section II) also applies to these networks, where the energy functions mini-  
 373 mized at equilibrium are the co-content, the inductive energy and the capacitive co-energy, respec-  
 374 tively ([15, 25]).

375 To emphasize the generality of Freq-prop, we present it here in the context of *central force spring*  
 376 *networks* (or ‘elastic networks’) ([5]), as well as Hopfield networks (the Ising model).

377 **a. Central force spring networks.** We consider an elastic network of  $N$  nodes interconnected  
 378 by springs. The elastic energy stored in the spring connecting node  $i$  to node  $j$  is  $E_{ij}(r_{ij}) =$   
 379  $\frac{1}{2}k_{ij}(r_{ij} - \ell_{ij})^2$ , where  $k_{ij}$  is the spring constant,  $\ell_{ij}$  is the spring’s length at rest, and  $r_{ij}$  is the  
 380 distance between nodes  $i$  and  $j$ . Nonlinear springs are also allowed and their energy terms are  
 381 gathered in a unique term  $E_{\text{nonlinear}}(r)$ . Thus, the total elastic energy stored in the network, which  
 382 is minimized, is given by

$$E(\theta, r) = \frac{1}{2} \sum_{i,j} k_{ij} (r_{ij} - \ell_{ij})^2 + E_{\text{nonlinear}}(r), \quad (\text{B1})$$

383 where  $\theta = \{k_{ij}, \ell_{ij}\}$  is the set of adjustable parameters, and  $r = \{r_{ij}\}$  plays the role of state  
 384 variable.

385 In this setting as in the case of resistive networks, we apply a nudging signal  $\gamma \sin(\omega t) C(r, y)$  at  
 386 the output part of the network, we observe the response  $r(t)$ , and we assume that we can recover the  
 387 first two vectors of Fourier coefficients of  $r(t)$ , i.e. the vectors  $a$  and  $b$  such that  $a = \frac{1}{T} \int_0^T r(t) dt$   
 388 and  $b = \frac{2}{T} \int_0^T r(t) \sin(\omega t) dt$ . Then, the learning rules for the spring constant  $k_{ij}$  and the spring’s  
 389 length at rest  $\ell_{ij}$  read, in this context,

$$\Delta k_{ij} = -\alpha b_{ij} (a_{ij} - \ell_{ij}), \quad \Delta \ell_{ij} = -\alpha k_{ij} b_{ij}. \quad (\text{B2})$$

390 Theorem 2 generalizes to this setting ; the above learning rules perform stochastic gradient descent  
 391 on the loss:  $\Delta \theta = -\alpha \gamma \frac{\partial \mathcal{L}}{\partial \theta}(\theta, x, y) + O(\gamma^3)$ .

392 **b. Continuous Hopfield networks.** Freq-prop also applies to Hopfield networks (the Ising  
 393 model) ([11, 26]). In a Hopfield network of multiple units interconnected by synapses, the en-  
 394 ergy term between unit  $i$  and unit  $j$  is  $E_{ij} = w_{ij} h_i h_j$ , where  $w_{ij}$  is the synaptic weight, and  $h_i$  is  
 395 the state of unit  $i$ . The total energy is

$$E(\theta, h) = \frac{1}{2} \sum_{i,j} w_{ij} h_i h_j, \quad (\text{B3})$$

396 where  $\theta = \{w_{ij}\}$  is the set of adjustable parameters, and  $h = \{h_i\}$  plays the role of state variable.  
 397 After applying a nudging signal  $\gamma \sin(\omega t) C(h, y)$  at a set of output units, we observe the response  
 398  $u(t)$  (the state of the units at equilibrium), we compute the vectors  $a$  and  $b$  such that  $a = \frac{1}{T} \int_0^T u(t) dt$   
 399 and  $b = \frac{2}{T} \int_0^T u(t) \sin(\omega t) dt$ . The learning rules for the weight  $w_{ij}$  reads

$$\Delta w_{ij} = -\alpha (a_i b_j + a_j b_i), \quad (\text{B4})$$

400 which performs stochastic gradient descent on the loss, up to  $O(\gamma^3)$ .

## 401 Appendix C: Related Work

402 Frequency propagation builds on learning via *chemical signaling* ([1]), which is another example  
 403 of multi-mechanism learning (MmL) in physical networks. Whereas MmL via frequency propa-  
 404 gation uses two different frequencies to play the role of the *activation* and *error* signals during  
 405 training, MmL via chemical signaling uses two different chemical concentrations for these signals.

406 [1] presents learning via chemical signaling in the setting of linear flow networks, which we extend  
407 here to the nonlinear setting (Appendix D).

408 Freq-prop is also related to *equilibrium propagation* (EP) ([3, 12]) and *coupled learning* ([5]).  
409 To see the relationship with these algorithms, we consider the case of resistive networks (sec-  
410 tion II). Denote  $v_{jk} = v_j - v_k$  the voltage across branch  $(j, k)$ . Further denote  $v^\beta =$   
411  $\arg \min_v [E(\theta, x, v) + \beta C(v, y)]$  for any  $\beta \in \mathbb{R}$ . Based on a result from [12], [3] proved that  
412 the learning rule

$$\Delta^{\text{EP}} \theta_{jk} = \frac{\alpha}{2} \left( (v_{jk}^0)^2 - (v_{jk}^\beta)^2 \right) \quad (\text{C1})$$

413 performs gradient descent with step size  $\alpha\beta$ , up to  $O(\beta^2)$ . We note that the right-hand side of  
414 (C1) is also equal to  $\alpha v_{jk}^0 (v_{jk}^0 - v_{jk}^\beta) + O(\beta^2)$ , showing that the gradient information is con-  
415 tained in the physical quantities  $v^0$  and  $\left. \frac{\partial v^\beta}{\partial \beta} \right|_{\beta=0}$ . These quantities correspond to the activation  
416 and error signals of Freq-prop, respectively. To avoid the use of finite differences to measure  
417  $\left. \frac{\partial v^\beta}{\partial \beta} \right|_{\beta=0}$ , Freq-prop makes use of a time-varying nudging signal  $\beta(t) = \gamma \sin(\omega t)$ . With this  
418 method, the activation and error signals are encoded in the frequencies 0 and  $\omega$  of the response  
419 signal  $v(t) = v^0 + \gamma \sin(\omega t) \left. \frac{\partial v^\beta}{\partial \beta} \right|_{\beta=0} + O(\gamma^3)$ . The required information can thus be recovered via  
420 frequency analysis.

421 The idea of using an oscillating nudging signal was also proposed by [11] and more recently (con-  
422 currently to our work) in ‘holomorphic EP’ ([27]). Our work differs from these two other works in  
423 several ways. First, our learning rule can be decomposed as ‘activation signal’ times ‘error signal’  
424 ( $a \times b$ ), whereas the learning rule of [11] takes the form  $\Delta \theta_{jk} = \frac{\alpha}{2} \int \sin(\omega t) v_{jk}(t)^2 dt$ , and simi-  
425 larly for holomorphic EP. Second, our learning rule is proved to approximate the gradient of the cost  
426 function, up to  $O(\beta^3)$ , unlike in [11]. In [27], the authors exploit the Cauchy formula of complex  
427 calculus to prove that their algorithm computes the exact gradient of the cost function, indepen-  
428 dently of the strength of the nudging signal. To achieve this, the authors allow the nudging factor  
429 to take complex values, i.e.  $\beta = \gamma e^{i\omega t} \in \mathbb{C}$ , and the domain of definition of the energy function  
430  $v \mapsto E(\theta, x, v)$  is extended to complex configurations  $v \in \mathbb{C}^N$ . However, it is not straightforward to  
431 see how this mathematical formalism can be directly mapped to physical systems such as resistive  
432 networks or spring networks, which is the motivation of our work.

433 Another very recent work proposes an alternative approach to train physical systems by gradient  
434 descent called *agnostic equilibrium propagation* ([8]). However, this method imposes constraints  
435 on the nature of the parameters  $(\theta)$ , which must minimize the system’s energy  $(E)$ , just like the  
436 state variables  $(v)$  do. This assumption does not allow us to view the conductances of resistors  
437 as trainable parameters in a resistive network. The method also requires control knobs with the  
438 ability to perform homeostatic control over the parameters. Our work can also be seen as a physical  
439 implementation of *implicit differentiation* in physical networks. We refer to ([28]) for a description  
440 of implicit differentiation where the authors use a mathematical formalism close to ours.

441 Lastly, other physical learning algorithms that make explicit use of time are being developed. For  
442 instance, recent work proposes a way to train physical systems with time reversible Hamiltonians  
443 ([6]). In this method called *Hamiltonian echo backpropagation* (HEB), the error signal is a time-  
444 reversed version – an “echo” – of the activation signal, with the cost function acting as a perturbation  
445 on this signal. However, HEB requires a feasible way to time-reverse the activation signal.

## 446 Appendix D: Multi-Mechanism Learning via Chemical Signaling

447 In this appendix, we generalize the learning algorithm via *chemical signaling* ([1]) to nonlinear net-  
448 works. Learning via chemical signaling is another example of *multi-mechanism learning* in physical  
449 networks. It uses pressures and chemical concentrations to implement a local learning rule. This way  
450 of using multiple independent “mechanisms” is the central idea behind multi-mechanism learning.

451 Consider a flow network, i.e. a network of nodes interconnected by tubes. A flow network is  
452 formally equivalent to the resistive network of Section II, with  $v$  being the configuration of node  
453 pressures, and  $\theta_{jk}$  being the conductance of the branch between nodes  $j$  and  $k$ .

454 Learning via chemical signaling proceeds as follows. In the first phase, given  $\theta$  and input signals  $x$ ,  
455 the configuration of node pressures stabilizes to its equilibrium value  $v(\theta, x)$  given by

$$v(\theta, x) = \arg \min_v E(\theta, x, v). \quad (\text{D1})$$

456 In the second phase, we inject chemical currents  $e = -\beta \frac{\partial C}{\partial v}(v(\theta, x), y)$  at output nodes, where  
457  $\beta$  is a (positive or negative) constant. As a result, a chemical concentration  $u$  develops at each  
458 node. Assuming that the configuration of node pressures  $v(\theta, x)$  is not affected by the chemical, the  
459 chemical concentration  $u$  at equilibrium satisfies the relationship:

$$\frac{\partial^2 E}{\partial v^2}(\theta, x, v(\theta, x)) \cdot u = -\beta \frac{\partial C}{\partial v}(v(\theta, x), y). \quad (\text{D2})$$

460 Indeed, diffusion along a tube follows the same equation as that of flow along the same tube, up  
461 to a constant factor (replacing node pressures and flow conductivity by chemical concentration and  
462 diffusion constant, respectively). When there is no ambiguity from the context, we write  $v = v(\theta, x)$   
463 for simplicity. We note that, although  $v$  is not affected by the chemical,  $u$  depends on  $v$ . In particular  
464  $u$  also depends on  $\theta$  and  $x$  through  $v$ .

465 Next, denoting  $u = (u_1, u_2, \dots, u_N)$ , we update each parameter  $\theta_{jk}$  according to the learning rule

$$\Delta \theta_{jk} = -\alpha (u_j - u_k) \cdot (v_j - v_k), \quad (\text{D3})$$

466 where  $\alpha$  is some constant. Note that this learning rule is local (just like the learning rule of Freq-  
467 prop), requiring only information about nodes  $j$  and  $k$  for each conductance  $\theta_{jk}$ .

468 **Theorem 4** For every parameter  $\theta_{jk}$ , it holds that

$$\Delta \theta_{jk} = -\alpha \beta \frac{\partial \mathcal{L}}{\partial \theta_{jk}}(\theta, x, y). \quad (\text{D4})$$

469 Namely, the learning rule of Eq. (D3) performs one step of gradient descent with respect to the loss,  
470 with step size  $\alpha\beta$ . We note that learning via chemical signaling comes in two variants, either with  
471  $\beta > 0$  and  $\alpha > 0$ , or with  $\beta < 0$  and  $\alpha < 0$ . The procedure performs one step of gradient *descent*  
472 as long as the product  $\alpha\beta$  is positive.

473 [Proof of Theorem 4] First, we write the first-order equilibrium condition for  $v(\theta, x)$ , which is

$$\frac{\partial E}{\partial v}(\theta, x, v(\theta, x)) = 0. \quad (\text{D5})$$

474 We differentiate this equation with respect to  $\theta$ :

$$\begin{aligned} \frac{\partial^2 E}{\partial v^2}(\theta, x, v(\theta, x)) \frac{\partial v}{\partial \theta}(\theta, x) + \\ \frac{\partial^2 E}{\partial v \partial \theta}(\theta, x, v(\theta, x)) = 0. \end{aligned} \quad (\text{D6})$$

475 Multiplying both sides on the left by  $u^\top$  we get

$$\begin{aligned} u^\top \frac{\partial^2 E}{\partial v^2}(\theta, x, v(\theta, x)) \frac{\partial v}{\partial \theta}(\theta, x) + \\ u^\top \frac{\partial^2 E}{\partial v \partial \theta}(\theta, x, v(\theta, x)) = 0. \end{aligned} \quad (\text{D7})$$

476 On the other hand, multiplying both sides of (D2) on the left by  $\frac{\partial v}{\partial \theta}(\theta, x)^\top$ , we get

$$\begin{aligned} \frac{\partial v}{\partial \theta}(\theta, x)^\top \frac{\partial^2 E}{\partial v^2}(\theta, x, v(\theta, x)) u \\ = -\beta \frac{\partial v}{\partial \theta}(\theta, x)^\top \frac{\partial C}{\partial v}(v(\theta, x), y) \\ = -\beta \frac{\partial \mathcal{L}}{\partial \theta}(\theta, x, y) \end{aligned} \quad (\text{D8})$$

477 Comparing (D7) and (D8) we conclude that

$$u^\top \frac{\partial^2 E}{\partial v \partial \theta}(\theta, x, v(\theta, x)) = \beta \frac{\partial \mathcal{L}}{\partial \theta}(\theta, x, y). \quad (\text{D9})$$

478 Finally, using the form of the energy function (2), we have for each parameter  $\theta_{ij}$

$$(u_i - u_j) \cdot (v_i - v_j) = \beta \frac{\partial \mathcal{L}}{\partial \theta_{ij}}(\theta, x, y). \quad (\text{D10})$$

479 Therefore the learning rule

$$\Delta \theta_{jk} = -\alpha (u_i - u_j) \cdot (v_i - v_j) \quad (\text{D11})$$

480 satisfies

$$\Delta \theta_{jk} = -\alpha \beta \frac{\partial \mathcal{L}}{\partial \theta_{jk}}(\theta, x, y). \quad (\text{D12})$$

481 Hence the result.